Nonlinear Dynamics and Systems Theory, **19** (3) (2019) 405–415

State Estimation of Rotary Inverted Pendulum Using HOSM Observers: Experimental Results

F. A. Haouari [1], Q. V. Dang [2], J.-Y. Jun [3], M. Djemai [2*] and B. Cherki [1]

[1] *Department of Electrical Engineering and Electronics, Tlemcen University, Algeria*
[2] *LAMIH, UMR CNRS 8201; UVHC, 59313 Valenciennes, France*
[3] *Sorbonne University, UPMC Univ Paris 06, UMR 7222, ISIR, F-75005, Paris, France*

Received: December 23, 2018; Revised: June 26, 2019

Abstract: This paper presents the observer design for the state estimation of the rotary inverted pendulum (RIP) system. A Takagi-Sugeno (T-S) fuzzy descriptor approach is used for modeling the nonlinear dynamic system. Two higher-order sliding mode (HOSM) observers, based on the super-twisting algorithm, are proposed and applied to the RIP with real-time implementation. The experimental results illustrate the finite-time convergence and accuracy of the state estimates of the designed observers.

Keywords: *rotary inverted pendulum; T-S fuzzy descriptor model; super-twisting algorithm; higher-order sliding mode observer.*

Mathematics Subject Classification (2010): 93B07, 93C10, 93C42, 93C85.

1 Introduction

Recently, sliding mode techniques have been widely used for the problems of dynamic systems control and observation due to their finite-time convergence and robustness against various kinds of uncertainties such as parameter perturbations and external disturbances [1]. In particular, higher-order sliding mode (HOSM) based observers can be considered as a successful technique for the state observation of perturbed systems, due to their high precision and robust behavior with respect to parametric uncertainties [13]. In [7], the step-by-step first-order sliding mode observers are designed for a class of systems in triangular input form. Nevertheless, the realization of first-order sliding mode implies the undesirable chattering phenomena.

Many observers, based on the high-order sliding mode technique, have been developed

* Corresponding author: mailto:mohamed.djemai@univ-valenciennes.fr

recently for a class of nonlinear systems. The high-order sliding mode is used to overcome the chattering phenomena occurring. In [2]- [6], the HOSM observers based on an exact and robust sliding mode differentiator of order 2 (a super-twisting algorithm) have been proposed. The super-twisting algorithm (STA) is one of the most popular second-order sliding mode algorithms which offer a finite-time and exact convergence and it has been widely used for control and observation [13]. The robustess, better accuracy and finite-time convergence of these observers can be used for the state estimation and fault diagnosis of uncertain nonlinear dynamics systems.

In this paper, the synthesis of an iterative sliding mode observer for the state estimation of the RIP system using the super-twisting algorithm is presented, when the angular velocities are not measured directly. As an underactuated and unstable system, the rotary inverted pendulum system has been regarded as an attractive test platform for linear and nonlinear control law verification since Katsuhisa Furuta, Professor at the Tokyo Institute of Technology, introduced it to the feedback control community in 1992 [11]. Also, it has some significant real-life applications such as the position control, aerospace vehicles control, and robotics [14]. Here, the modeling of the RIP system is based on T-S fuzzy descriptor systems [9]. The T-S fuzzy systems have been proven to be a powerful tool for modeling and controlling complex systems [8]. Recently, the fuzzy T-S representation in a descriptor form has generated a great interest in control systems design. The descriptor system describes a wider class of systems including physical models and nondynamic constraints [9] and using the fuzzy descriptor system can reduce the number of LMI conditions for controller design [10].

This paper is structured as follows. In Section 2, the description and T-S fuzzy descriptor model of the RIP system are given. Section 3 presents the design procedure and convergence analysis of the proposed HOSM observers. Section 4 provides experimental results. The final Section 5 concludes this paper.

2 Rotary Inverted Pendulum System

2.1 Mathematical model

A schematic of the rotary inverted pendulum is represented in Fig. 1 [12]. The system consists of a servo-motor which runs a gear to rotate a pendulum arm of radius r which in turn affects the motion of a pendulum rod of length l and mass m. The plane of the pendulum is orthogonal to the radial arm. Let ϕ be the angle of the pendulum rod from the upright position about the x_1-axis and θ be the rotational angle of the pendulum arm about the vertical axis z.

The mathematical model of the RIP is derived from the Euler-Lagrange equations which are obtained from an energy analysis of the system [12]. The nonlinear model is represented by a set of dynamical equations given as follows:

$$\begin{cases} \frac{4}{3}c_1\ddot{\phi} + c_2\ddot{\theta}cos\phi - c_1\dot{\theta}^2 sin\phi\, cos\phi + c_3\dot{\phi} - c_4 sin\phi = 0, \\ c_2\ddot{\phi}cos\phi + (c_5 + c_1 sin^2\phi)\ddot{\theta} - c_2\dot{\phi}^2 sin\phi + c_6\dot{\theta} + 2c_1\dot{\phi}\dot{\theta}sin\phi\, cos\phi = c_7 V_m, \end{cases} \tag{1}$$

where

$$c_1 = \frac{ml^2}{4},\ c_2 = \frac{mlr}{2},\ c_3 = B_r,\ c_5 = J_{eq} + mr^2 + \eta_g K_g^2 J_m,$$
$$c_4 = \frac{mgl}{2},\ c_7 = \frac{\eta_m\eta_g K_t K_g}{R},\ c_6 = B_a + \frac{\eta_m\eta_g K_t K_v K_g^2}{R},$$

V_m is the control input voltage applied on the motor. For the definition of notations used for the constants, see Table 2.

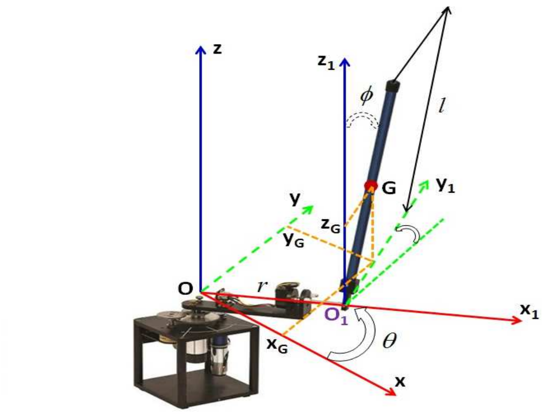

Figure 1: Schematic of the rotary inverted pendulum (upright position).

2.2 Descriptor T-S model

Introducing the variables $x_1 = \phi$, $x_2 = \theta$, $x_3 = \dot{\phi}$, $x_4 = \dot{\theta}$, the input $u = V_m$ and the measured output $y = [\phi, \theta]^T$, the pendulum model (1) can be written in a regular descriptor form

$$\begin{cases} E(x)\dot{x}(t) = A(x)x(t) + Bu(t), \\ y(t) = Cx(t), \end{cases} \tag{2}$$

where $x = [x_1 x_2 x_3 x_4]^T$ is the state vector,

$$E(x) = \begin{bmatrix} 1 & 0 & 0 & 0 \\ 0 & 1 & 0 & 0 \\ 0 & 0 & \frac{4}{3}c_1 & c_2 cos\phi \\ 0 & 0 & c_2 cos\phi & c_5 + c_1 sin^2\phi \end{bmatrix}, \quad B = \begin{bmatrix} 0 \\ 0 \\ 0 \\ c_7 \end{bmatrix},$$

$$A(x) = \begin{bmatrix} 0 & 0 & 1 & 0 \\ 0 & 0 & 0 & 1 \\ c_4 \frac{sin\phi}{\phi} & 0 & -c_3 & \alpha \\ 0 & 0 & \beta & -c_6 \end{bmatrix}, \quad C = \begin{bmatrix} 1 & 0 & 0 & 0 \\ 0 & 1 & 0 & 0 \end{bmatrix}$$

with $\alpha = c_1\dot{\theta} sin\phi cos\phi$ and $\beta = c_2\dot{\phi} sin\phi - 2c_1\dot{\theta} sin\phi cos\phi$.

Consider n_e and n_a being the numbers of nonlinear terms contained in the matrices $E(x)$ and $A(x)$, respectively. Then, the descriptor T-S fuzzy model is described by a set of $r_e \times r_a = 2^{n_e} \times 2^{n_a} = 32$ linear models, with $n_e = 2$ and $n_a = 3$. In order to simplify the model, the nonlinearities α and β are taken into account as bounded uncertainties. This allows reducing the number of linear models from 32 to 8.

Thus 3 nonlinearities are under consideration and specify a state dependent premise vector, $z(t)$. The premise variables $z_j(t)$, $j = 1, ..., 3$, are given by

$$z_1 = c_2 cos(\phi), \quad z_2 = c_5 + c_1 sin^2\phi, \quad z_3 = c_4 \frac{sin(\phi)}{\phi}. \tag{3}$$

Therefore, through the local sector nonlinearities approach [9], the nonlinear dynamics model of the RIP can be approximated by the following fuzzy T-S representation in a descriptor form

$$\begin{cases} \sum_{k=1}^{r_e} v_k(z(t)) E_k \dot{x}(t) = \sum_{i=1}^{r_a} w_i(z(t))(A_i x(t) + Bu(t)), \\ y(t) = Cx(t), \end{cases} \tag{4}$$

where $r_e = 4$, $r_a = 2$, and both nonlinear functions $v_k(z(t)) \geq 0$, $k \in \{1, ..., r_e\}$, $w_i(z(t)) \geq 0$, $i \in \{1, ..., r_a\}$ satisfy the convex sum property, i.e. $\sum_{k=1}^{r_e} v_k(z(t)) = 1$ and $\sum_{i=1}^{r_a} w_i(z(t)) = 1$.

Consider $\overline{z_j}$ (resp. $\underline{z_j}$) being the maximum (resp. minimum) of z_j, the premise variables $z_j(t)$, $j = 1, ..., 3$, can be written as

$$z_j(t) = M_{j1}(z_j(t))\overline{z_j} + M_{j2}(z_j(t))\underline{z_j} \tag{5}$$

with

$$M_{j1}(z_j(t)) = (z_j - \underline{z_j})/(\overline{z_j} - \underline{z_j}), \quad M_{j2}(z_j(t)) = (\overline{z_j} - z_j)/(\overline{z_j} - \underline{z_j}), \tag{6}$$

where

$$M_{j1}(z_j(t)) + M_{j2}(z_j(t)) = 1. \tag{7}$$

Then, the system matrices have the expressions

$$E_1 = \begin{bmatrix} 1 & 0 & 0 & 0 \\ 0 & 1 & 0 & 0 \\ 0 & 0 & \frac{4}{3}c_1 & \overline{z_1} \\ 0 & 0 & \overline{z_1} & \overline{z_2} \end{bmatrix}, \; E_2 = \begin{bmatrix} 1 & 0 & 0 & 0 \\ 0 & 1 & 0 & 0 \\ 0 & 0 & \frac{4}{3}c_1 & \overline{z_1} \\ 0 & 0 & \overline{z_1} & \underline{z_2} \end{bmatrix},$$

$$E_3 = \begin{bmatrix} 1 & 0 & 0 & 0 \\ 0 & 1 & 0 & 0 \\ 0 & 0 & \frac{4}{3}c_1 & \underline{z_1} \\ 0 & 0 & \underline{z_1} & \overline{z_2} \end{bmatrix}, \; E_4 = \begin{bmatrix} 1 & 0 & 0 & 0 \\ 0 & 1 & 0 & 0 \\ 0 & 0 & \frac{4}{3}c_1 & \underline{z_1} \\ 0 & 0 & \underline{z_1} & \underline{z_2} \end{bmatrix},$$

$$A_1 = \begin{bmatrix} 0 & 0 & 1 & 0 \\ 0 & 0 & 0 & 1 \\ \overline{z_3} & 0 & -c_3 & 0 \\ 0 & 0 & 0 & -c_6 \end{bmatrix}, \; A_2 = \begin{bmatrix} 0 & 0 & 1 & 0 \\ 0 & 0 & 0 & 1 \\ \underline{z_3} & 0 & -c_3 & 0 \\ 0 & 0 & 0 & -c_6 \end{bmatrix},$$

$v_k(z(t)) \geq 0$, $k \in \{1, ..., r_e\}$, $w_i(z(t)) \geq 0$, $i \in \{1, ..., r_a\}$. Therefore, the functions $v_k(z(t)) \geq 0$, $k \in \{1, ..., 4\}$, and $w_i(z(t)) \geq 0$, $i \in \{1, 2\}$, are obtained by

$$\begin{aligned} & w_1(z) = M_{31}(z_3);\ w_2(z) = M_{32}(z_3), \\ & v_1(z) = M_{11}(z_1) \times M_{21}(z_2);\ v_2(z) = M_{11}(z_1) \times M_{22}(z_2), \\ & v_3(z) = M_{12}(z_1) \times M_{21}(z_2);\ v_4(z) = M_{12}(z_1) \times M_{22}(z_2). \end{aligned} \tag{8}$$

The set of 8 model rules is given in Table 1.

The control law used to stabilize the RIP in the upright position is the robust T-S descriptor stabilizing controller proposed in [12], which stabilizes the system in the

Table 1: Rules of T-S fuzzy descriptor model for the RIP.

	Membership functions			***Matrices***
Rules	$\mathbf{M_{1j}(z_1)}$	$\mathbf{M_{2j}(z_2)}$	$\mathbf{M_{3j}(z_3)}$	$\mathbf{E_k,A_i}$
1	M_{11}	M_{21}	M_{31}	E_1,A_1
2	M_{11}	M_{21}	M_{32}	E_1,A_2
3	M_{11}	M_{22}	M_{31}	E_2,A_1
4	M_{11}	M_{22}	M_{32}	E_2,A_2
5	M_{12}	M_{21}	M_{31}	E_3,A_1
6	M_{12}	M_{21}	M_{32}	E_3,A_2
7	M_{12}	M_{22}	M_{31}	E_4,A_1
8	M_{12}	M_{22}	M_{32}	E_4,A_2

operating range under uncertainties and distrubances. Then, the control input $u(t)$ is a fuzzy parallel distributed compensation (PDC) [12]:

$$u(t) = \sum_{k=1}^{4}\sum_{i=1}^{2} w_i(z(t))v_k(z(t))K_{ik}x(t) \tag{9}$$

with the following feedback gain matrices:

$$\begin{array}{rl}
K_{11} = & [26.8550 \quad 1.4142 \quad 3.8231 \quad 2.0844], \\
K_{12} = & [25.1416 \quad 1.4142 \quad 3.5734 \quad 2.0638], \\
K_{13} = & [41.6885 \quad 1.4142 \quad 6.0852 \quad 2.0945], \\
K_{14} = & [39.0849 \quad 1.4142 \quad 5.7014 \quad 2.0741], \\
K_{21} = & [24.9747 \quad 1.4142 \quad 3.7940 \quad 2.1137], \\
K_{22} = & [23.4523 \quad 1.4142 \quad 3.5580 \quad 2.0932], \\
K_{23} = & [38.7119 \quad 1.4142 \quad 6.0174 \quad 2.1233], \\
K_{24} = & [36.3931 \quad 1.4142 \quad 5.6539 \quad 2.1029].
\end{array} \tag{10}$$

The observability of the system (4) requires that all the subsystems are observable, consider the following assumption.

Assumption 2.1 The system (4) satisfies the following rank test conditions for observability, ($k = 1, ..., r_e$ and $i = 1, ..., r_a$) [15]:

$$rank \begin{bmatrix} sE_k - A_i \\ C \end{bmatrix} = n, \ \forall s \in \mathbb{C}, \tag{11}$$

$$rank \begin{bmatrix} E_k & A_i \\ 0 & E_k \\ 0 & C \end{bmatrix} = n + rank(E_k). \tag{12}$$

The objective of this paper is to design finite-time convergent observers of the velocities $\dot{\phi}$ and $\dot{\theta}$ for the RIP system, when only the positions ϕ and θ are measurable. The state vector x is estimated with the second-order sliding mode observers proposed in the following section.

3 Second-Order Sliding Mode Observer Design

3.1 Step-by-step sliding mode of order 2

Consider the sliding mode differentiator of order 2 (the super-twisting algorithm) [5]

$$\begin{cases} u(e_1) = u_1 + \lambda_1 |e_1|^{\frac{1}{2}} sign(e_1), \\ \dot{u}_1 = \alpha_1 sign(e_1), \end{cases} \tag{13}$$

where $e_1 = x_1 - \hat{x}_1$, and λ_1 and α_1 are positive tuning parameters of the differentiator whose output is u_1. The *sign* function is approximated by the saturation function with a high gain in the boundary layer. An important feature of the differentiator (13) is the fact that the output does not depend directly on discontinuous functions, but on an integrator output. So, high-frequency chattering is attenuated [5].

First, let us consider system (4). It can be rewritten into two subsystems in a triangular observable form as follows:

$$\Sigma_1 = \begin{cases} \dot{x}_1 = x_3, \\ \dot{x}_3 = \frac{3}{4c_1}(cx_1 - a\dot{x}_4 - c_3 x_3) = f_1(t,x), \\ y_1 = x_1, \end{cases} \tag{14}$$

$$\Sigma_2 = \begin{cases} \dot{x}_2 = x_4, \\ \dot{x}_4 = \frac{1}{b}(c_7 u - c_6 x_4 - a\dot{x}_3) = f_2(t,x,u), \\ y_2 = x_2. \end{cases} \tag{15}$$

with

$$\begin{aligned} a &= (v_1(z) + v_2(z))\overline{z_1} + (v_3(z) + v_4(z))\underline{z_1}, \\ b &= (v_1(z) + v_3(z))\overline{z_2} + (v_2(z) + v_4(z))\underline{z_2}, \\ c &= w_1(z)\overline{z_3} + w_2(z)\underline{z_3}. \end{aligned}$$

Applying the super-twisting algorithm (13) to the transformed system (14)-(15), the step-by-step sliding mode observers (Σ_{obs1}) and (Σ_{obs2}) are obtained, respectively, as

$$\Sigma_{obs1} = \begin{cases} \dot{\hat{x}}_1 = \tilde{x}_3 + \lambda_1 |x_1 - \hat{x}_1|^{\frac{1}{2}} sign(x_1 - \hat{x}_1), \\ \dot{\tilde{x}}_3 = \alpha_1 sign(x_1 - \hat{x}_1), \\ \dot{\hat{x}}_3 = \tilde{\theta}_1 + F_1 \lambda_2 |\tilde{x}_3 - \hat{x}_3|^{\frac{1}{2}} sign(\tilde{x}_3 - \hat{x}_3), \\ \dot{\tilde{\theta}}_1 = F_1 \alpha_2 sign(\tilde{x}_3 - \hat{x}_3), \end{cases} \tag{16}$$

$$\Sigma_{obs2} = \begin{cases} \dot{\hat{x}}_2 = \tilde{x}_4 + \lambda_3 |x_2 - \hat{x}_2|^{\frac{1}{2}} sign(x_2 - \hat{x}_2), \\ \dot{\tilde{x}}_4 = \alpha_3 sign(x_2 - \hat{x}_2), \\ \dot{\hat{x}}_4 = \tilde{\theta}_2 + F_2 \lambda_4 |\tilde{x}_4 - \hat{x}_4|^{\frac{1}{2}} sign(\tilde{x}_4 - \hat{x}_4), \\ \dot{\tilde{\theta}}_2 = F_2 \alpha_4 sign(\tilde{x}_4 - \hat{x}_4), \end{cases} \tag{17}$$

where $\hat{x}_i$, $i = 1, ..., 4$, are the state estimates and the functions F_i, $i = 1, 2$, are given by $F_i = 0$ if $e_i > \epsilon$, otherwise $F_i = 1$, where ϵ is a small positive constant.

Suppose that the system (14) is BIBS (Bounded Inputs Bounded State) in finite time, then the functions f_1, f_2 and their first-time derivatives are bounded by the known constants, for all $t > 0$,

$$\begin{aligned} |f_1| &< K_1, \qquad |\dot{f}_1| < K_2, \\ |f_2| &< K_3, \qquad |\dot{f}_2| < K_4. \end{aligned} \tag{18}$$

3.2 Convergence analysis

Consider the system (14) and the HOSM observer (16). Let us define the estimation errors as $e_i = \tilde{x}_i - \hat{x}_i$, $i = 1, ..., 4$, with $\tilde{x}_1 = x_1$ and $\tilde{x}_2 = x_2$.

Lemma 3.1 *For any initial conditions $(x_1(0), x_3(0))$, $(\hat{x}_1(0), \hat{x}_3(0))$ there exists a choice of λ_i and α_i such that the observer state $(\hat{x}_1, \hat{x}_3)$ converges in finite time to (x_1, x_3).*

Proof. The convergence of the observation error is obtained in one step in finite time.
Step 1: Assume $e_1(0) \neq 0$, the error dynamics is given by

$$\begin{cases} \dot{e}_1 = x_3 - \tilde{x}_3 - \lambda_1 |e_1|^{\frac{1}{2}} sign(e_1), \\ \dot{\tilde{x}}_3 = \alpha_1 sign(e_1), \\ \dot{e}_3 = f_1 - \tilde{\theta}_1 - F_1 \lambda_2 |e_3|^{\frac{1}{2}} sign(e_3). \end{cases}$$

The second time derivative of e_1 is given by

$$\ddot{e}_1 = f_1 - \alpha_1 sign(e_1) - \frac{1}{2}\lambda_1 \dot{e}_1 |e_1|^{-\frac{1}{2}}. \tag{19}$$

From [6], the sufficient conditions for the finite-time convergence on the second-order sliding set $\{e_1 = \dot{e}_1 = 0\}$ are

$$\begin{aligned} &\alpha_1 > K_1, \\ &\lambda_1 > \sqrt{2}\frac{K_1 + \alpha_1}{\sqrt{\alpha_1 - K_1}}. \end{aligned} \tag{20}$$

The finite-time convergence to the second-order sliding set ensures that there exists a time $t_1 > 0$ such that for all $t > t_1$: $\hat{x}_1 = x_1$ and $\tilde{x}_3 = x_3$.
Step 2: For $t > t_1$, $F_1 = 1$ and the observer dynamics becomes

$$\begin{cases} \dot{e}_1 = 0, \\ \dot{e}_3 = f_1 - \tilde{\theta}_1 - \lambda_2 |e_3|^{\frac{1}{2}} sign(e_3), \\ \dot{\tilde{\theta}}_1 = \alpha_2 sign(e_3). \end{cases}$$

The second time derivative of e_3 has the form

$$\ddot{e}_3 = \dot{f}_1 - \alpha_2 sign(e_3) - \frac{1}{2}\lambda_2 \dot{e}_3 |e_3|^{-\frac{1}{2}}. \tag{21}$$

Thus, a sliding motion appears after a finite time on the sliding manifold $\{e_3 = \dot{e}_3 = 0\}$. The observer gains satisfy [6]

$$\begin{aligned} &\alpha_2 > K_2, \\ &\lambda_2 > \sqrt{2}\frac{K_2 + \alpha_2}{\sqrt{\alpha_2 - K_2}}. \end{aligned} \tag{22}$$

Therefore, in the sliding mode, there exists a time $t_2 > t_1$ such that for all $t > t_2$: $\hat{x}_3 = \tilde{x}_3$ and $\dot{\tilde{\theta}}_1 = (\alpha_2 sign(e_3))_{eq}$.

According to a similar convergence analysis of the observer (16), the sufficient conditions of the observer (17) for the finite-time convergence to the sliding manifold $\{e_i = \dot{e}_i = 0\}$, $i = 2, 4$, are

$$\begin{aligned} &\alpha_3 > K_3, \\ &\lambda_3 > \sqrt{2}\frac{K_3 + \alpha_3}{\sqrt{\alpha_3 - K_3}}, \end{aligned} \tag{23}$$

$$\begin{aligned} &\alpha_4 > K_4, \\ &\lambda_4 > \sqrt{2}\frac{K_4 + \alpha_4}{\sqrt{\alpha_4 - K_4}}. \end{aligned} \tag{24}$$

Thus, the convergence of the observer states $(\hat{x}_2, \hat{x}_4)$ from (17) to the system state variables (x_2, x_4) in (15) occurs in finite time. □

4 Experimental Results

Experimental results of the proposed observers (16) and (17) are presented in this section. A picture of the experimental setup of the considered RIP system is shown in Fig.2. The different parts include: a rotary inverted pendulum manufactured by Quanser, a VoltPAQ-X2 linear voltage amplifier, a PC with measurement computing PCI-QUAD04 quadrature encoder board and PCI-DAS6025 board. The development of the controller and observer systems is made in the MATLAB/Simulink environment. The numerical values of the mechanical and electrical system parameters for the RIP-model are provided in Table 2.

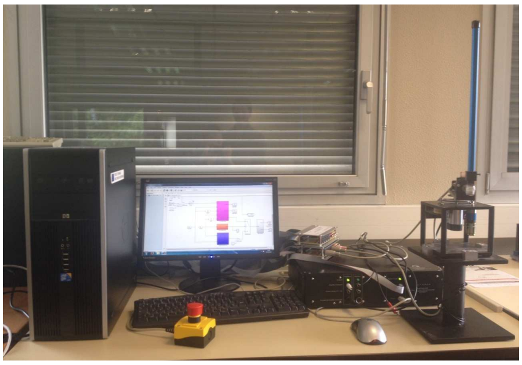

Figure 2: The experiment setup.

The T-S fuzzy descriptor system (4) approximates the RIP system in a range of $|\phi| \leq \phi_0$. For $\phi_0 = \frac{49\pi}{180}$ (rad), it follows that

$$\begin{aligned} \underline{z}_1 &= 0.003, & \underline{z}_2 &= 0.0111, & \underline{z}_3 &= 0.1813, \\ \overline{z}_1 &= 0.0045, & \overline{z}_2 &= 0.0131, & \overline{z}_3 &= 0.2054, \end{aligned} \tag{25}$$

and the state equation matrices are

$$E_1 = \begin{bmatrix} 1 & 0 & 0 & 0 \\ 0 & 1 & 0 & 0 \\ 0 & 0 & 0.0047 & 0.0045 \\ 0 & 0 & 0.0045 & 0.0131 \end{bmatrix}, \quad E_2 = \begin{bmatrix} 1 & 0 & 0 & 0 \\ 0 & 1 & 0 & 0 \\ 0 & 0 & 0.0047 & 0.0045 \\ 0 & 0 & 0.0045 & 0.0111 \end{bmatrix},$$

$$E_3 = \begin{bmatrix} 1 & 0 & 0 & 0 \\ 0 & 1 & 0 & 0 \\ 0 & 0 & 0.0047 & 0.003 \\ 0 & 0 & 0.003 & 0.0131 \end{bmatrix}, \quad E_4 = \begin{bmatrix} 1 & 0 & 0 & 0 \\ 0 & 1 & 0 & 0 \\ 0 & 0 & 0.0047 & 0.003 \\ 0 & 0 & 0.003 & 0.0111 \end{bmatrix},$$

$$A_1 = \begin{bmatrix} 0 & 0 & 1 & 0 \\ 0 & 0 & 0 & 1 \\ 0.2054 & 0 & -0.001 & 0 \\ 0 & 0 & 0 & -0.0729 \end{bmatrix},$$

$$A_2 = \begin{bmatrix} 0 & 0 & 1 & 0 \\ 0 & 0 & 0 & 1 \\ 0.1813 & 0 & -0.001 & 0 \\ 0 & 0 & 0 & -0.0729 \end{bmatrix}, \quad B = \begin{bmatrix} 0 \\ 0 \\ 0 \\ 0.1282 \end{bmatrix}.$$

Table 2: The mechanical and electrical system parameters [12].

Symbol	***Description***	***Value***
m	Mass of the pendulum rod (kg)	0.125
l	Length of the pendulum rod (m)	0.335
r	Length of the pendulum arm (m)	0.215
J_{eq}	Equivalent moment of inertia of the pendulum arm and gears (kgm^2)	3.5842×10^{-3}
J_m	Moment of inertia of the motor rotor (kgm^2)	3.87×10^{-7}
B_a	Friction coefficient of the pendulum arm ($Nmsrad^{-1}$)	0.004
B_r	Friction coefficient of the pendulum rod ($Nmsrad^{-1}$)	0.0095
g	Gravity (ms^{-2})	9.81
K_t	Torque constant (NmA^{-1})	7.67×10^{-3}
K_v	Back EMF constant ($Vsrad^{-1}$)	7.67×10^{-3}
R	Motor armature resistance (Ω)	2.6
K_g	Gearbox ratio	70
η_g	Gearbox efficiency	0.9
η_m	Motor efficiency	0.69

It is assumed that the pendulum starts in the stable downward position. First, the swing up control [12] swings the pendulum up till it reaches the inverted position. When the pendulum rod is within $\pm\phi_0$, it can then be caught in the upright position with the robust T-S fuzzy descriptor controller (9).

The initial values of the estimated states are $\hat{x}$=$[0\,0\,0\,0]^T$. The proposed HOSM observers (16) and (17) estimate the positions and velocities of the RIP. The observer gains are selected as in (20), (22)- (24) to ensure the convergence of the observers. The chosen gains λ_1, α_1, λ_2, α_2, λ_3, α_3, λ_4 and α_4 are 40, 1500, 200, 3000, 40, 1500, 200, and 3000, respectively. The behavior of the proposed observers is shown by the following experimental results. Fig. 3 shows the convergence of the estimated positions θ_{est}, ϕ_{est} to the real positions θ_{mes}, ϕ_{mes}, respectively. Fig. 4 shows the estimates of velocities $\hat{\dot{\theta}}$

and $\hat{\dot{\phi}}$. The results indicate the finite-time convergence and accuracy of estimates of the proposed observers.

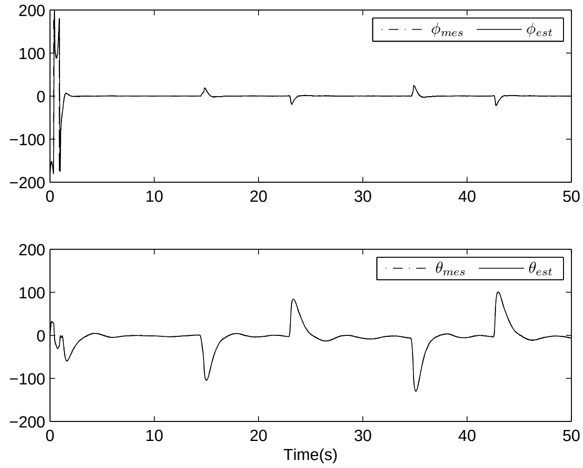

Figure 3: Pendulum rod's position (above) and pendulum arm's position (below): measured (dash-dotted), estimated (solid).

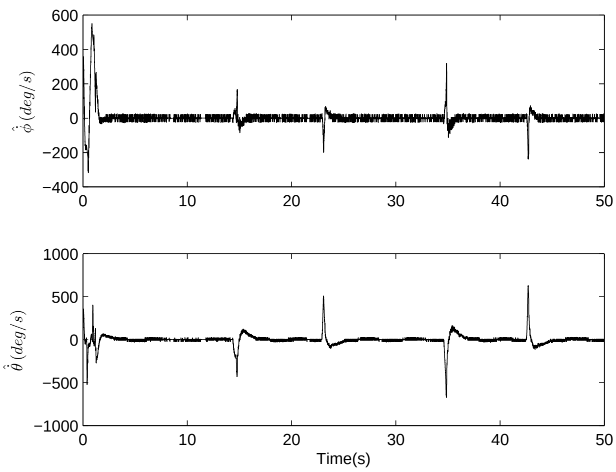

Figure 4: Pendulum rod's velocity estimate (above) and pendulum arm's velocity estimate (below).

Also, as is seen in Fig. 3, the RIP control system demonstrates good performance and maintains the pendulum in the upright position. The robustness is successfully realized by the robust T-S fuzzy descriptor controller in the presence of disturbances at time instants 14.4 s, 23 s, 34.6 s and 42.5 s. The oscillatory behavior observed in Fig. 4 is due to the backlash in the motor's gearbox.

5 Conclusion

This paper considers the state estimation of the T-S fuzzy descriptor system using a high-order sliding mode technique. Two second-order sliding mode observers based on the super-twisting algorithm have been proposed to reconstruct the states. The finite-time convergence and accuracy of estimates are demonstrated through experiments on a real-time example of the rotary inverted pendulum system.

References

[1] S. V. Drakunov and V. Utkin. Sliding Mode Observers, Tutorial. In: *Proc. Decision and Control Conf.* New Orleans, LA, 1995, 3376–3378.

[2] J.-P. Barbot and T. Floquet. Iterative higher order sliding mode observer for nonlinear systems with unknown inputs. *Dynamics of Continuous, Discrete and Impulsive Systems* **17** (6) (2010) 1019–1033.

[3] J. Davila, L. Fridman and A. Levant. Second-Order Sliding-Mode Observer for Mechanical Systems. *IEEE Transactions on Automatic Control* **50** (11) (2005).

[4] H. Rios, J. Davila and L. Fridman. High-order sliding mode observers for nonlinear autonomous switched systems with unknown inputs. *Journal of the Franklin Institute* **349** (10) (2012) 2975–3002.

[5] H. Saadaoui, N. Manamanni, M. Djemai, J.P. Barbot and T. Floquet. Exact differentiation and sliding mode observers for switched Lagrangian systems. *Nonlinear Analysis* **65** (2006) 1050–1069.

[6] T. Floquet and J.-P. Barbot. Super twisting algorithm based step-by-step sliding mode observers for nonlinear systems with unknown inputs. *International Journal of Systems Science* **38** (10) (2007).

[7] J.-P. Barbot, T. Boukhobza and M. Djemai. Sliding mode observer for triangular input form. In: *Proc. Decision and Control Conf.* Kobe, Japan, 2006.

[8] T. Takagi and M. Sugeno. Fuzzy identification of systems and its applications to modeling and control. *IEEE Transactions on SMC* **15** (1985) 116–132.

[9] K. Tanaka and H. O. Wang. *Fuzzy Control Systems and Design Analysis: A Linear Matrix Inequality Approach.* John Wiley & Sons, Inc, 2001.

[10] T. Taniguchi, K. Tanaka, and H. O. Wang. Fuzzy Descriptor Systems and Nonlinear Model Following Control. *IEEE Transactions on Fuzzy Systems* **8** (4) (2000) 442–452.

[11] K. Furuta, M. Yamakita, and S. Kobayashi. Swing-up control of inverted pendulum using pseudo-state feedback. *Journal of Systems and Control Engineering* **206** (6) (1992) 263–269.

[12] Q. V. Dang, B. Allouche, L. Vermeiren, A. Dequidt and M. Dambrine. Design and implementation of a robust fuzzy controller for a rotary inverted pendulum using the Takagi-Sugeno descriptor representation. In: *16th IFAC WC* Prague, Czech Republic, 2005.

[13] Y. Shtessel, C. Edwards, L. Fridman and A. Levant. *Sliding Mode Control and Observation.* Control Engineering, Springer, 2014.

[14] A. Choukchou-Braham, B. Cherki, M. Djemai and K. Busawon. *Analysis and Control of Underactuated Mechanical Systems.* Springer, Verlag, 2013.

[15] H. Hamdi, M. Rodrigues, C. Mechmeche and N. Benhadj Braiek. Observer based Fault Tolerant Control for Takagi-Sugeno Nonlinear Descriptor systems. In: *Proc. Control, Engineering & Information Technology Conf.*, 2013, 52–57.